An experimental investigation into the comparative hygrothermal performance of wall panels incorporating wood fibre, mineral wool and hemp-lime

E. Latif [a,*], R. M. H. Lawrence [b], A. D. Shea [b], P. Walker [b]

[a]Welsh School of Architecture, Cardiff University, Cardiff, CF10 3NB, UK

[b]BRE Centre for Innovative Construction Materials, Department of Architecture and Civil Engineering, University of Bath, BA2 7AY, UK

Abstract

Three wall panels of identical calculated U-value were simultaneously assessed in a large dual environmental chamber under a number of steady state and dynamic hygrothermal boundary conditions. This study used large-scale wall elements under identical controlled conditions in order to eliminate uncontrollable variables normally encountered in full-scale studies. The following panels were tested: Mineral Wool Panel, Wood Fibre Panel and the Biond Panel (an assembly of wood fibre and hemp-lime). Within the limits of the error range of the calculation, the measured U-value was same for all test panels when assessed under steady state and dynamic hygrothermal boundary conditions. It was however observed that in a boundary condition simulating intermittent heating, the Biond panel showed the highest heat storing and releasing capability whereas the Mineral Wool Panel showed the lowest. In terms of moisture management, the Biond panel exhibited the highest moisture dampening ability within the panel structure. Higher thermal and hygric inertia of the Biond panel may be useful in mitigating overheating of dwellings and reducing interstitial condensation.

Key words: Mineral Wool; Wood Fibre; Biond; U-value; bio-based insulation materials; hemp-lime; thermal conductivity; moisture.

1. Introduction

Buildings employ both passive and active methods to regulate the indoor environment. Both approaches contribute to the reduction in embodied and operational energy. Active strategies pursue optimisation of the control and operation of efficient building services systems, whilst passive strategies focus on the energy saving potential of the building fabric and fenestration through, for example, optimised orientation, glazing ratios, and better use of insulation materials [1]. Green building rating tools such as

* Corresponding author. E-mail address: latife@cardiff.ac.uk (E. Latif).

BREEAM (Building Research Establishment Environmental Assessment Method) [2] LEED (Leadership in Energy and Environmental Design) [3], and CASBEE (Comprehensive Assessment System for Building Environmental Efficiency) [4] have proposed adopting passive technologies at the initial stages of design development [5]. Voluntary standards such as Passive House [6] and Minergie-P [7] also promote a fabric-first approach through high fabric thermal performance, low U-values, minimal thermal bridging, and significantly reduced fabric air permeability, relative to that often permitted in local and national building codes. These rating tools and standards emphasise the importance of manufacturing building envelopes that carry low embodied energy and offer high energy saving potential. The increasing rate of carbon emission and resource depletion puts sustainability and operational performance to the fore in selecting insulation materials for building envelope [8]. Some rating schemes, e.g., BREEAM In-Use [9], and all European Commission member states have developed assessment methods and certification schemes, e.g., Display Energy Certificates [10], for the evaluation of post-occupancy operational energy. Accordingly, in order to sustain professional reputations and to meet the targeted levels of CO_2 emissions, it is vitally important that building envelope systems perform to their predicted level with regards to building operational energy use. However, post-occupancy evaluations have revealed that, in many instances, actual energy use in buildings is far in excess of the predicted performance [11-13]. This phenomenon is largely described as the ‘energy performance gap’ [14]. Some causes of ‘energy performance gap’ are recognised as inaccurate estimation of energy use, low construction quality, inadequate building services, mismatch between the specification and the actual construction details, occupants’ behaviour and the ‘Rebound Effect’ where actual energy use is less than what is expected due to behaviour adjustment of

the economic agent [15-17]. The risk of overheating the UK buildings with regards to future weather scenario and the role of the materials with high thermal inertia is well documented [18-20]. As such, the current paper concerns with the thermal and hygric performance of three wall panels with bio-based and mineral materials as the key constituents.

1.1. Previous studies

Hygrothermal performance of wall panels has been studied by a number of researchers using climate chambers, e.g., vapour open wall by Goto et al.[21], internal application of mineral wool on masonry walls by Pavlik and Černý [22], hemp-lime, concrete and brick wall panels by Arnaud [23], hemp fibre and mineral wool insulation by Latif et al. [24]. On the other hand, in-situ experimental studies have also been conducted to evaluate the hygric, thermal or hygrothermal performance of wall panels or insulation materials. For example, the comparison of hemp fibre insulation with mineral wool insulation by Latif et al. [25], thermal transmittance of cellulose and mineral wool insulation by Nicolajsen [26], interstitial condensation study of masonry walls with internal glass fibre insulation by Southern [27], thermal performance of insulation, board materials, inner linings and thermal paint on a historic brick wall by Walker and Pavia [28], hygrothermal performance of hemp-lime walls by Shea et al. [29], cross-laminated timber wall assemblies by McClung et al.[30], glass wool insulation by Stazi et al. [31], sheep wool insulation by Tucker et al. [32] and mineral wool insulation by Toman et al. [33]. While in-situ studies are useful in assessing the hygrothermal performance of envelope systems in real life scenarios, tests carried out in a climate chamber complement the findings of in-situ tests by focusing on certain hygric or thermal properties of the envelope system that requires less background noise and controlled hygrothermal boundary conditions during assessments.

1.2. The aim to the current study

The aim of the current article is to compare, in steady state and dynamic boundary conditions, the U-value, thermal inertia and hygric performance of a composite bio-based panel ('Biond') with two other mainstream wall panels in controlled hygrothermal boundary conditions. Two of the wall panels, Biond and Wood Fibre, contain bio-based materials, and the other wall panel contains mineral wool. The Biond panel [28] is a newly developed prefabricated timber-framed composite panel with hemp-lime and cellulose fibre (hemp or wood fibre) at the core. The panel attempts to utilise the excellent hygric and thermal mass and moderate thermal resistance of hemp-lime [34-38] and excellent thermal resistance and good hygric and thermal mass of hemp or wood fibre [25, 39] with the aim of improving the overall energy performance of the envelope systems. Because of prefabrication of the Biond panel, mass production is possible with better quality control and reduced wasted resources. Thus, prefabrication is an advantage over in-situ casting of hemp-lime since in-situ casting may result into inconsistent quality and performance due to the dependence on the skill of the builders and sourcing of the materials. The findings of the paper will inform on the potential thermal performance gap that may occur due the difference in steady state and dynamic hygrothermal boundary conditions. The findings will further inform on the thermal inertia of the selected wall panels.

2. Material and Method

2.1. Overview of the methodology

The U-value, thermal inertia and hygric performance of the wall panels are compared in controlled steady state and dynamic hygrothermal boundary conditions. The measured U-value and thermal capacity are furthered compared with the analytically determined design U-values and calculated thermal capacities.

All panels used in the experiment have the identical design/calculated U-value of 0.15 W/m^{2}K. Previously, tests were conducted in tests cells built of similar panels in a number of coheating tests as detailed in [40] that focused more on the overall energy use of the test buildings in steady state internal conditions. The current experiments use a large environmental chamber, installed in the Building Research Park, Wroughton, that allows wider range of controlled hygrothermal boundary conditions than those offered by coheating tests. The panels were installed alongside each other in a sample holder positioned between the two cells of the large environmental chamber.

2.2. Wall assemblies and instrumentation

Three wall assemblies, each having dimensions of 1.1 m X 1.1 m, incorporate the following insulation materials: Mineral Wool 1, Mineral Wool 2, Hemp-lime and Wood Fibre 1, Wood Fibre 2 and Wood Fibre 3. Table 1 presents the physical properties of the insulation materials. The details of the assemblies with instrumentation are shown in Figs.1-3.

Table 1. Key constituents of the insulation material of the wall assemblies.

Material	Key Constituents	Thickness (mm)	Density (kg/m^3)	Specific Heat Capacity (J/KgK)	Thermal Capacity J/m^{2}K	Thermal Conductivity (W/mK)	Thermal Resistance (m^{2}K/W)
Mineral Wool 1 [41]	Mineral wool	140	100	840	11760	0.035	4.00
Mineral Wool 2 [41]	Mineral wool	100	50	840	4200	0.035	2.86
Hemp-lime (measured properties)	Hemp shive, lime, drying additive	120	240	1700 [42]	48960	0.07	1.71
Wood fibre 1 [43]	Wood fibre	180	55	2100	20790	0.038	4.74
Wood Fibre 2 [44]	Wood fibre	60	140	2100	17640	0.038	1.58
Wood Fibre 3 [43]	Wood fibre	220	55	2100	25410	0.038	5.79
OSB [45]	Wood	9	650	1550	9067.5	0.13	0.07
Timber Stud [46]	Wood	Variable	470	1650	Variable	0.12	Variable
Plasterboard [47]	Gypsum	12.5	668	1090	9101.5	0.19	0.07
Air layer [48]	Air	25	1.2	1005	30.15	0.024	0.18 [49]

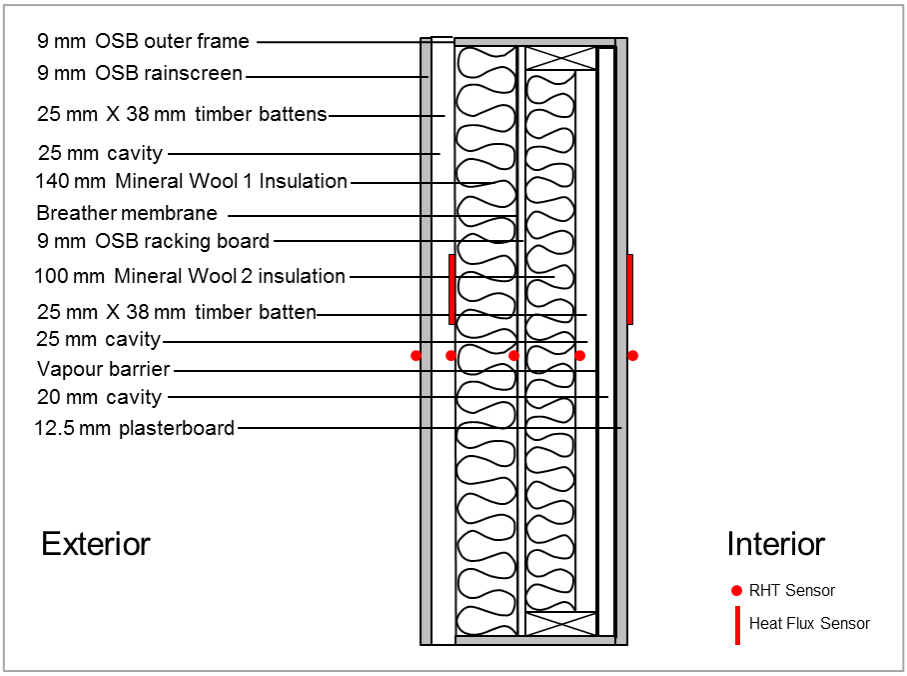

Fig. 1. Details and instrumentation of the Mineral Wool panel.

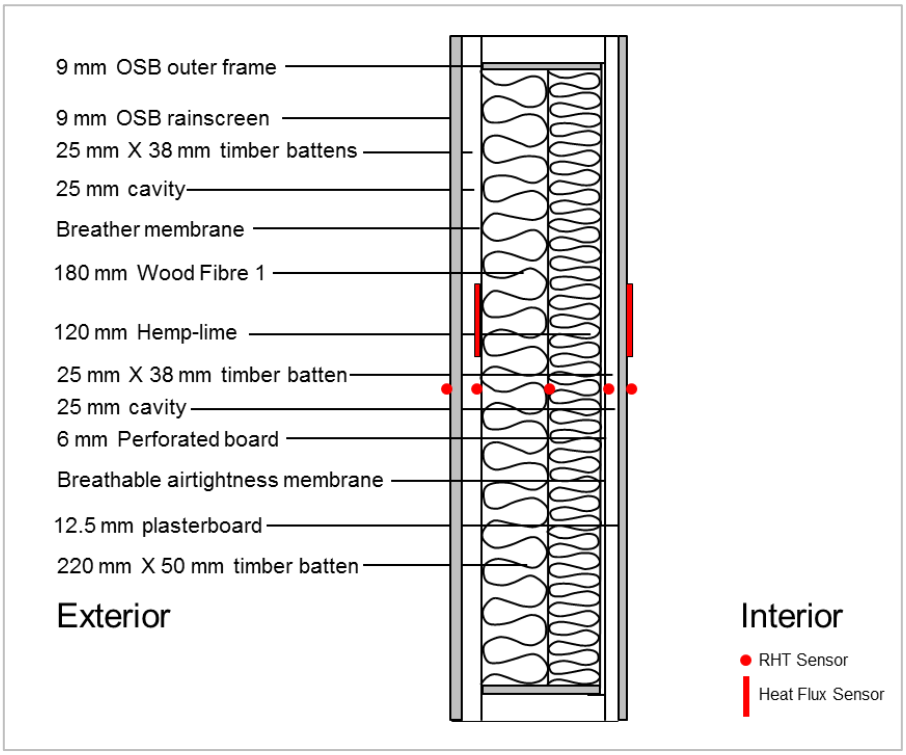

Fig. 2. Details and instrumentation of the Biond panel

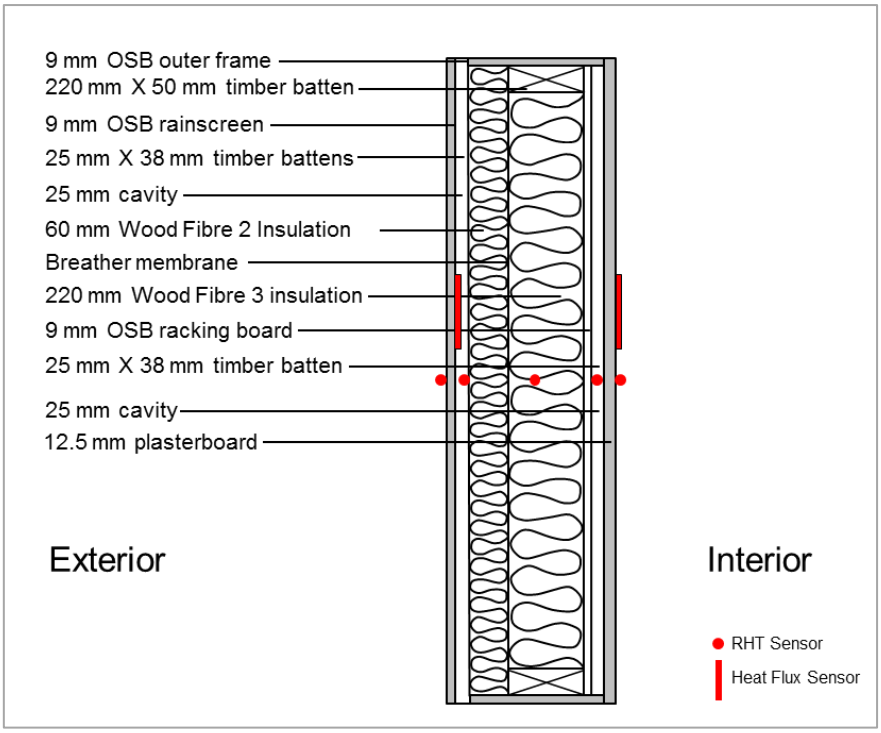

Fig. 3. Details and instrumentation of the Wood Fibre Panel

The wall panels are instrumented with five Campbell Scientific CS215 digital temperature and relative humidity sensors, five Type-T thermocouples and two Hukseflux heat flux sensors as presented in Figs. 1-3.

The CS215 sensor [50] is 180 mm in length with an average diameter of 15 mm. The accuracy of temperature measurement is ± 0.9 °C in the range of -40 °C to +70 °C. The accuracy of the relative humidity measurement is ±4% in the range of 0%-100% relative humidity at 25 °C. The Type T thermocouples have an accuracy of ± 1 °C or ± 0.75% (whichever is greater) and a range of -75-260 °C [51]. Hukseflux HFP01 heat flux sensors (Figs. 1-3) have the accuracy of ± 5% on walls and the measurement range of -2000 W/m^2 and +2000 W/m^2 [52]. The thickness of the sensor is 5 mm with a diameter of 80 mm. The wall panels have I joist timber/OSB studs at the middle and both ends. The heat flux sensors are placed in between two studs, using thermal paste, so that the effect of thermal bypass is considered.

2.3. The large Environmental Chamber

The Large Environmental Chamber (Fig. 4), situated at the Building Research Park, Wroughton, is formed of two highly insulated chambers. The dimensions of the chamber that represents the conditions of the indoor environment (Room 1) is 4 m x 4 m x 2.9 m. The dimensions of the chamber that represents the conditions of the outdoor environment (Room 2) is 3 m x 4 m x 2.9 m (Fig. 5). The test panel is placed in between the two sections of the chamber (Fig. 6). The temperature and humidity range of the environmental chamber during operation is presented in Table 2.

Table 2. The operation temperature and relative humidity range inside the environmental chamber.

	Room 1, Indoor	**Room 2, Outdoor**
Temperature range	5°C to 40 °C	-20°C to 40 °C
Relative Humidity Range	10%-95%	10%-95%
Stability in time	±1.0K or better and ±3% RH or better	±1.0K or better and ±3% RH or better
Stability in space	±2.0K or better and ±3% RH or better	±2.0K or better and ±3% RH or better

Fig. 4. The large environmental chamber.

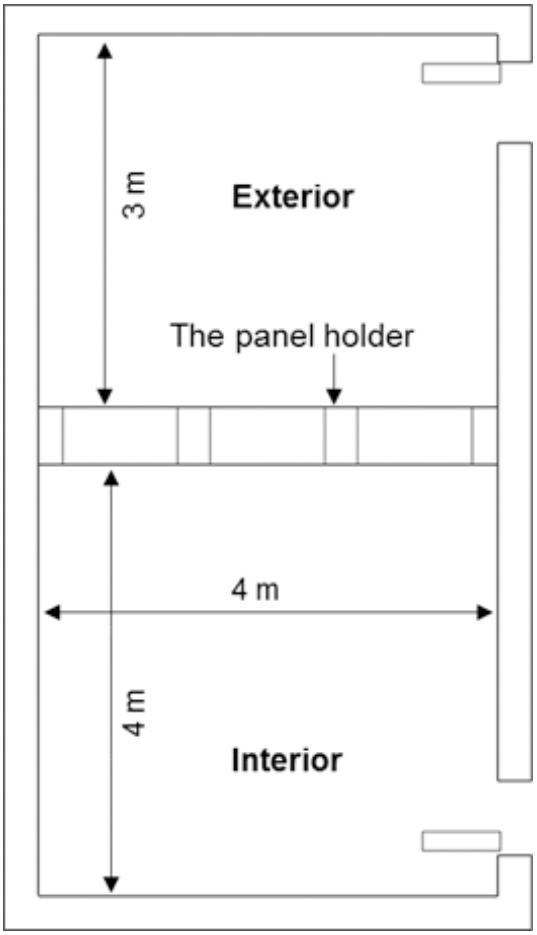

Fig. 5. The layout of the environmental chamber.

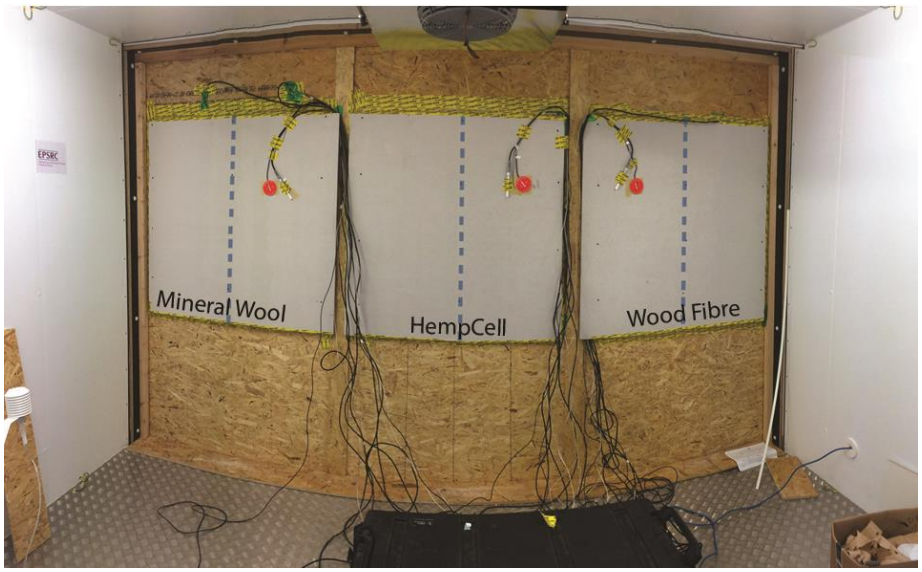

Fig. 6. The test panels in the environmental chamber.

2.4. The Hygrothermal protocol

Three test profiles were designed to assess the thermal performance, thermal inertia and hygric behaviour of the test panels in steady state and dynamic conditions. The steady state profile was based on the average internal and external temperature and relative humidity in the UK during the winter time. The dynamic test profiles were based on the average diurnal temperature and relative humidity during the winter. The profile was further simplified to address the limitations of the upper and lower limit of the combined temperature and relative humidity generation capacity of the large environmental chamber. The third profile was based on the changes in internal temperature only in such a way that the effect of thermal inertia could be quantified in terms of heat storage in the panels and heat release to the indoor. Therefore, there was no active moisture control during the third test. The profiles are described in detail in section 3.

2.5. Method of data analysis

2.5.1. Design U-value

The design U-value of the wall panels are calculated following BS EN ISO 6946:2017 [53]. The calculation methods are as follows,

U-value of wall panels of homogeneous layers:

The total thermal resistance, R_T, of a wall panel of thermally homogeneous layers perpendicular to the heat flow is:

$$R_T = R_{si} + R_1 + R_2 + \ldots + R_n + R_{se} \quad [1]$$

Where,

R_{si} The internal surface resistance

$R_1, R_2 \ldots R_n$ Thermal resistance of the layers

R_{se} The external surface resistance

U-value of wall panels of homogeneous and inhomogeneous layers:

R of a building component with homogeneous and inhomogeneous layers parallel to the surface is the average of the upper and lower limits of the resistance:

$$R_T = (R'_T + R''_T)/2 \quad [2]$$

Where,

R'_T The upper limit of total thermal resistance

R''_T The lower limit of total thermal resistance

For one-dimensional heat flow, R'_T is determined by:

$$1/ R'_T = f_a/ R_{Ta} + f_b/ R_{Tb} + \ldots + f_q/ R_{Tq} \quad [3]$$

Where,

$R_{Ta}, R_{Tb} \ldots R_{Tq}$ are the thermal resistances from environment to environment for each section, calculated using equation [1]

$f_a, f_b \ldots f_q$ are the fractional areas of each section.

The horizontal cross-section of a wall panel [54] is presented in Fig. 7, where a, b and c are the width of perpendicular sections and d1, d2, d3 are the thickness along the depth.

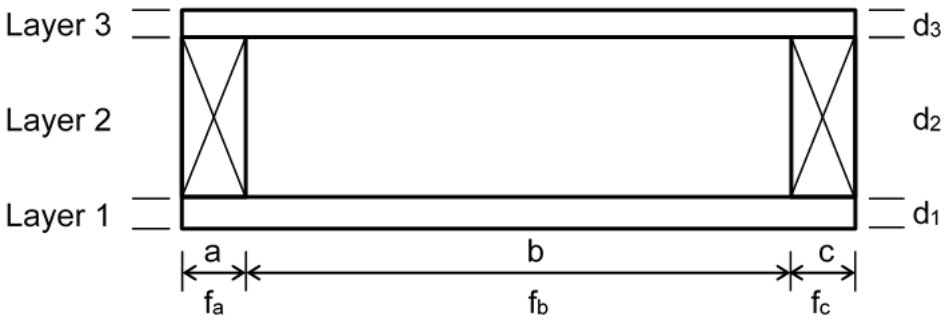

Fig.7 Horizontal cross-section of a notional wall panel [54]

For the determination of R''_T, it is assumed that all planes parallel to the surfaces are isothermal.

The equivalent thermal resistance, R_j, for thermally inhomogeneous layers is individually determined by,

$$1/ R_j = f_a/ R_{aj} + f_b/ R_{bj} + \ldots + f_q/ R_{qj} \quad [4]$$

Where:

R_{aj}, R_{bj}…….. R_{qj} are the thermal resistance of fractional areas f_a, f_b… f_q of layer j.

Finally, the lower limit of the thermal resistance is,

$$R''_T = R_{si} + R_1 + R_2 + \ldots + R_n + R_{se} \quad [5]$$

The error in thermal transmittance is:

$$e = ((R'_T - R''_T)*100)/ (2\ R_T) \quad [6]$$

2.5.2. In-situ U-value

U-values can be determined according to BS ISO 9869-1 [55] by dividing the average heat flux by the average temperature difference between the interior and the exterior.

The data are obtained for 72 hours or more for heavyweight structures and minimum three nights for lightweight structures. However, day/night variation is irrelevant for the tests inside the environmental chamber since solar radiation was not simulated. The equation for U-value is,

$$U = \frac{\sum_{j=1}^{n} q_j}{\sum_{j=1}^{n} (T_{ij} - T_{ej})} \quad [7]$$

Where:

U Thermal transmittance (W/m^2K)

Q Heat flux (W/m^2)

T_i Interior temperature (°C)

Te Exterior temperature (°C).

The computed asymptotical value will be close to the real value if the heat content in the panels is same at the beginning and end of the tests, and the heat flux sensors are not exposed to solar radiation.

According to BS ISO 9869-1 [55], heat flux measurement may have the following operational errors [56],

a. An error of 5% is attributable to the calibration of the heat flux sensor and the temperature.
b. An error of 5% is attributable to the inconsistency in thermal contact between the surface and the sensor. However, high conductance thermal paste has been used between the heat flux sensors and the surfaces. The error is assumed as 2%.
c. The operational error of 2-3% attributable to the change of temperature distribution for the installation of the heat flux sensors. An error of 2% is taken for the current experiment.
d. An error of 10% is attributable to the temporal variations of temperature and heat flux variation. The error is assumed as 8% for the current experiment since data were taken for sufficient period of time.
e. For U-value measurement, 5% error is suggested for the variation in radiant and air temperature and non-homogenous internal temperature distribution.

As such the cumulative error can be expressed as,

Cumulative error in U-value = $\sqrt{5^2 + 2^2 + 2^2 + 8^2 + 5^2}$ = 11 % [8]

2.5.3. Assessment of thermal inertia

2.5.3.1. Experimental analysis

Thermal inertia was assessed by comparing the amount of heat released by different wall panels to the interior and the amount of heat stored in the panels for an intermittent heating profile. As a comparative measure, the analysis was carried out in heat flux terms (W/m^2) and energy terms (KWh). The key steps of the analysis are as follows,

1. The outward heat flux from the inner surface and external surface (excluding the rain screen) were measured when internal temperature was higher than the external temperature. The difference between the two measurements represents the 'trapped heat' or 'heat sink' in the panels.
2. Inward heat flux was measured when internal temperature was going down from 30°C to 15°C and finally stayed at 15 °C while the external temperature remained constant at 15 °C. Since, the external temperature is planned to be higher than or equal to internal temperature, any internal heat gain from the wall will be due to their thermal mass.
3. The discrepancy between the 'heat sink' and the 'released heat' is calculated as the 'Heat retained in the system' since this remaining heat is not released back to the interior during the thermal cycle.

2.5.3.2. Analytical determination

Effective heat capacity is analytically assessed in terms of equivalent heat capacity [57], Thermal Time Constant [58] and effective thickness [59].

One of the simplified ways of comparing the thermal response of the wall panels is to analytically determine their equivalent heat capacity using the following equation [57]:

$$(\rho . c)_{eq} = \frac{1}{L} . \sum_{i=1}^{n} (\rho_i . c_i . \delta_i) \quad [9]$$

Where ρ is density (kg/m^3), c is specific heat capacity (J/KgK), L is the thickness of the wall panel, n is the number of layers in the wall panel, ρ_i is the density of a single layer, c_i is the heat capacity of a single layer and δ_i is the thickness (m) of a single layer of the wall panel.

Effective heat capacity is also determined from the Thermal Time Constant (TTC) [58]. TTC is defined as the sum of the individual products of thermal resistance and thermal capacity (areal heat capacity). The thermal resistance of each layer is calculated from the external surface up to the centre of the selected layer including the external surface resistance. Thus, assuming external surface resistance as 0.04 m^2k/W, the thermal resistance of the n^{th} layer is,

$R_n = r_0 + r_1 + r_2 + r_3 \ldots\ldots + 0.5*r_n$ [10]

And for an envelope with n layers,

$$\mathrm{TTC} = \sum_{i=1}^{n} (\rho_i . c_i . \delta_i . R_i) \quad [11]$$

Effective heat capacity of area A is derived from the following equation,

$$Q_m = A * \frac{\mathrm{TTC}}{R} \quad [12]$$

Where, R is the total thermal resistance of the selected envelope.

Annex C of BS EN ISO 13786 [59], for the purpose of simplified approximation of effective heat capacity, suggests the effective thickness of a wall component as 100 mm for the period of variations of one day. Effective heat capacity is expressed as,

$$(\rho . c)_{eq} = \sum_i (\rho_i . c_i . \delta_i) \quad [13]$$

Where, effective thickness = $\sum_i \delta_i$

3. Results and discussion

3.1. Winter steady state test

For the steady state test, internal temperature and relative humidity were set as 20°C and 60% and the external temperature and relative humidity were set as 5°C and 90%, respectively (Fig. 8). Thus, the target temperature difference was 15K, and the target vapour pressure difference was 6.2 Hectopascal (hPa). The measured 13-day test profile is presented in Fig. 9, the average temperature difference was 14.2K and the average vapour pressure difference was 5.4 hPa. The direction of vapour and heat flow was from the “interior” to the “exterior”. It can be noted that there is a spike in the time series in Fig. 9. The spike happened due to a temporary electric malfunction of the climate chambers. However, we analysed the data initially both with and without the spike and did not find any difference in the U-values as the effect was averaged out.

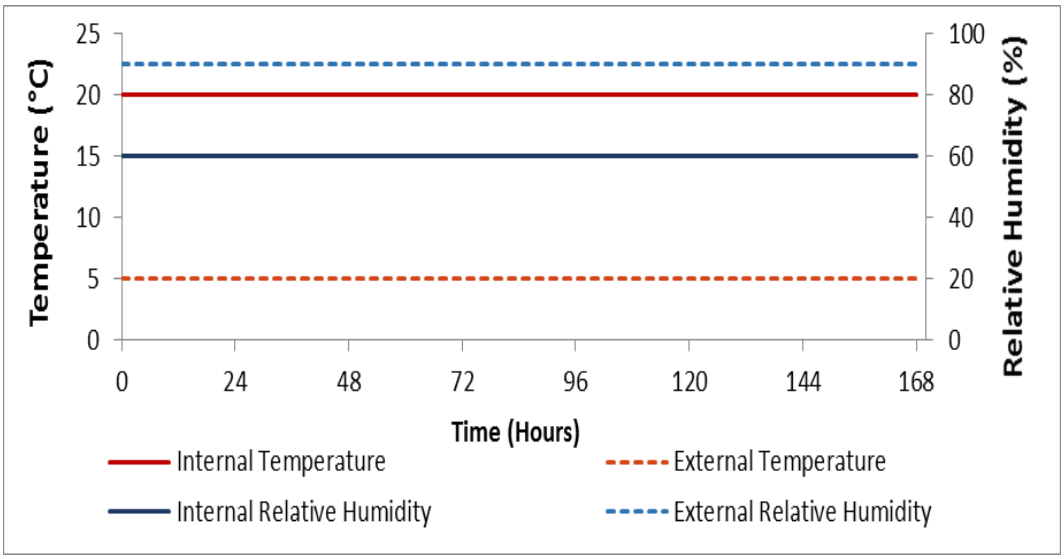

Fig. 8. The internal and external air to air temperature differences of the test cells.

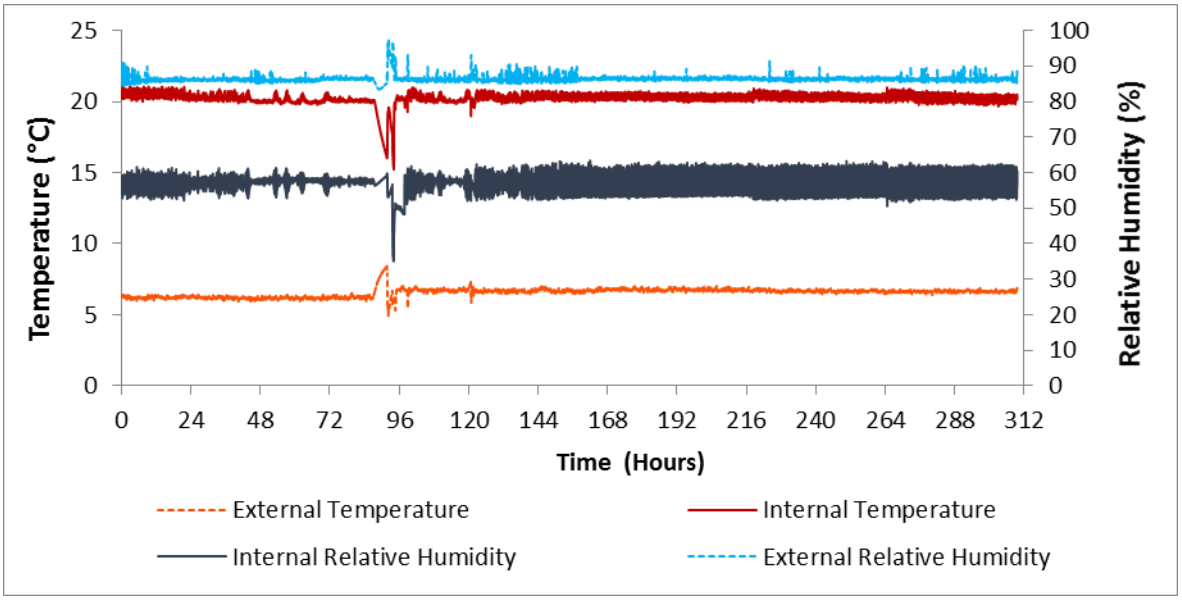

Fig. 9. The steady state hygrothermal profile in the environmental chamber.

From the hygrothermal profile attained in the environmental chamber, U-value of the panels was determined following ISO 9869. The running U-value and the average U-value of the panels are shown in Figs. 10 and 11, respectively. The results are within the error range of the designed U-value of the panels of 0.15 W/m^{2}K.

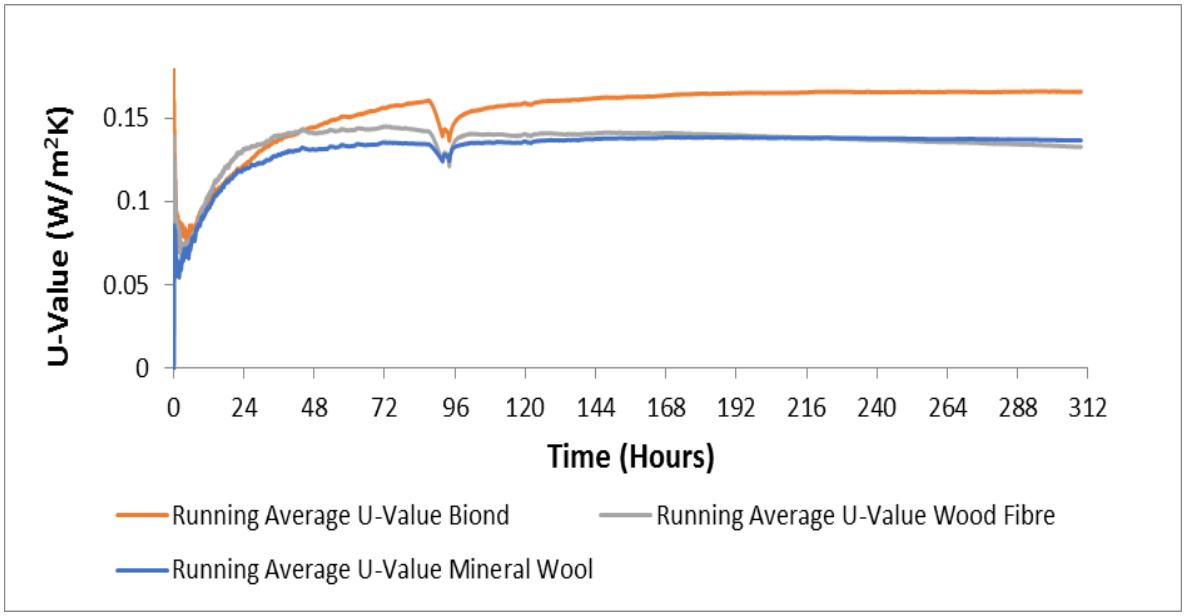

Fig. 10. The running U-value of the panels during the winter steady state test.

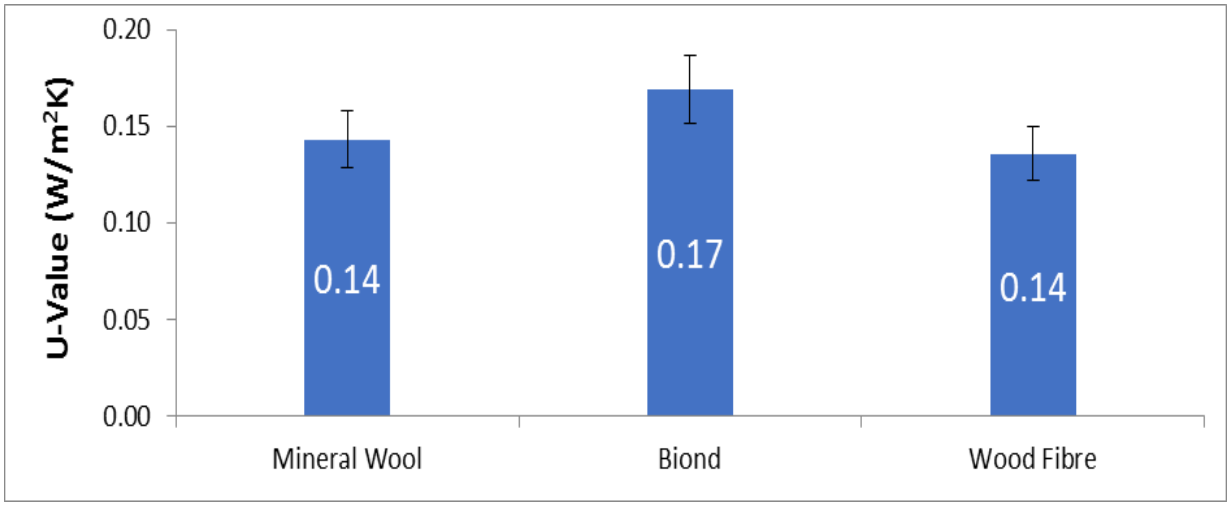

Fig. 11. The average U-value of the panels during the winter steady state test.

The evolution of vapour pressure and relative humidity in the centre of the panels was also assessed (Fig. 12). It can be observed that from the 10th hour, the relative humidity and vapour pressure within the Biond and Mineral Wool panels are nearly identical, within the measurement error range. For the same relative humidity, based on the data provided in [54, 60] and as compiled in Fig. 13, moisture adsorption by mass in Hemp-lime and Wood Fibre are higher than that in Mineral Wool by ten and twelve times, respectively. It implies that the increase of moisture content had a negligible effect on the dry thermal conductivity values of Biond and Wood Fibre panels during this experiment.

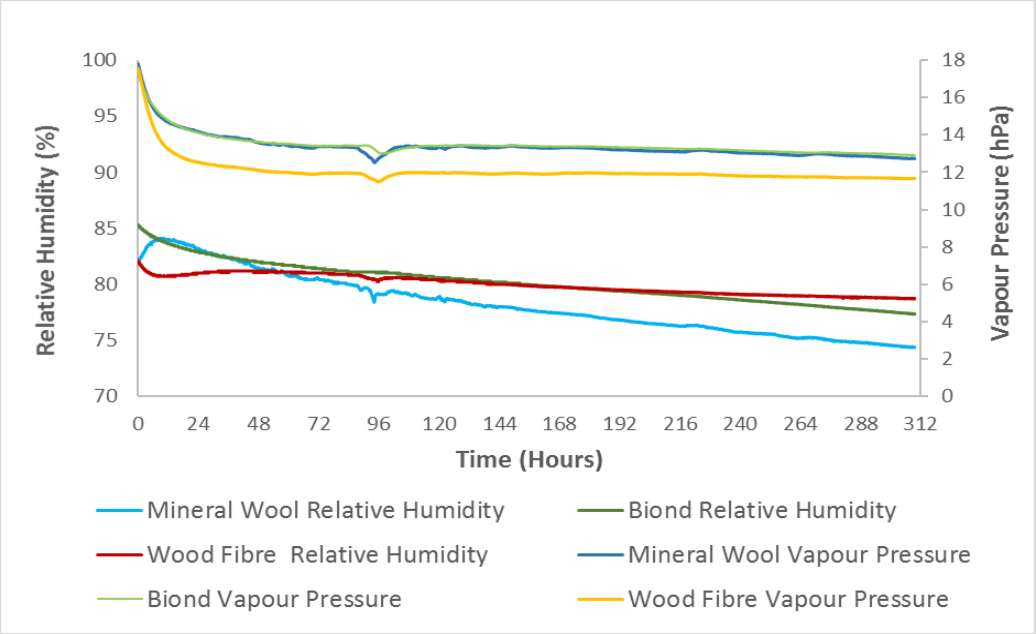

Fig.12. Relative humidity and vapour pressure in the centre of the panels.

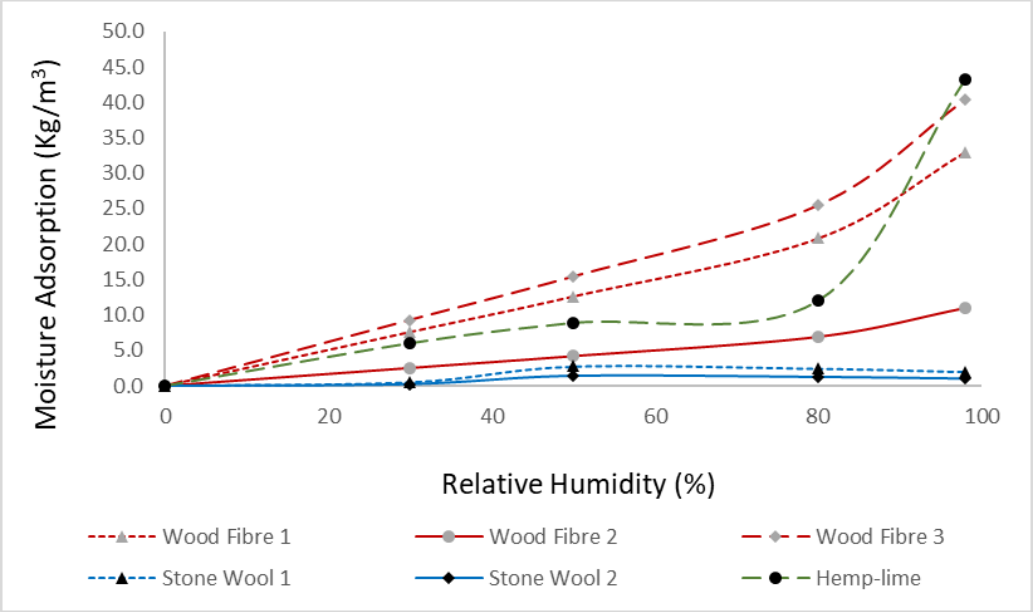

Figure 13. Adsorption isotherms of Stone Wool, Hemp-lime and Wood Fibre insulations.

3.2. Winter dynamic test

The designed hygrothermal profile for winter dynamic test is shown in Fig. 14. The internal temperature and relative humidity were kept constant at 20°C and 50% with a vapour pressure of 11.7 hPa. The external temperature and relative humidity

fluctuated between 15°C and 80% (vapour pressure 13.6 hPa) to 5°C and 90% (vapour pressure 7.8 hPa) at every 6 hours. Therefore, while the temperature gradient was always towards the exterior, the slope of vapour pressure gradient was changing at every six hours. The eight-day hygrothermal profile that was finally achieved by the environmental chamber is shown in Fig. 15.

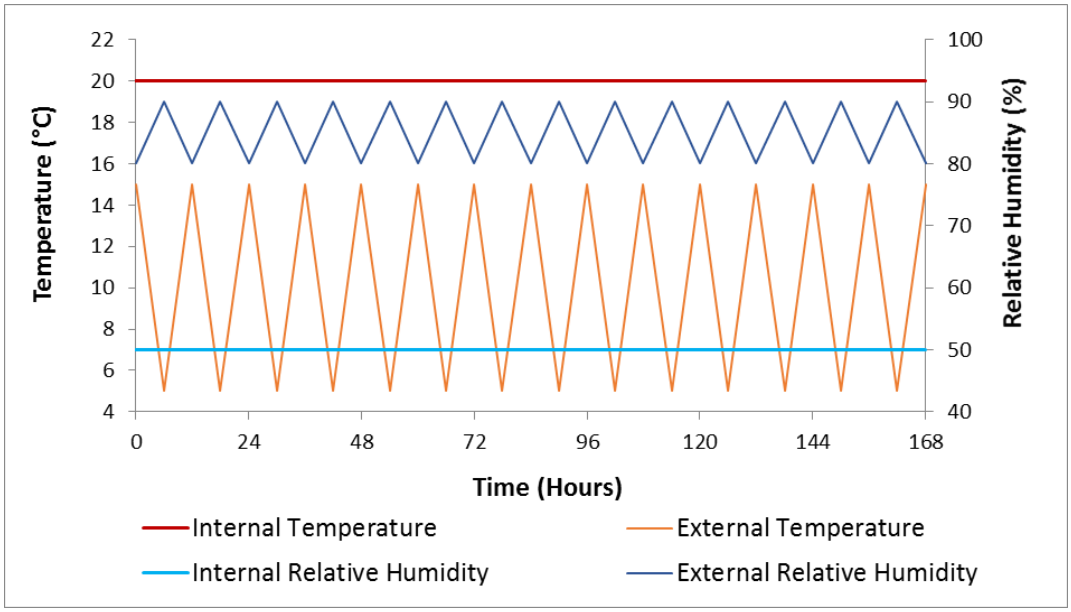

Fig. 14. The designed winter dynamic profile in the environmental chamber.

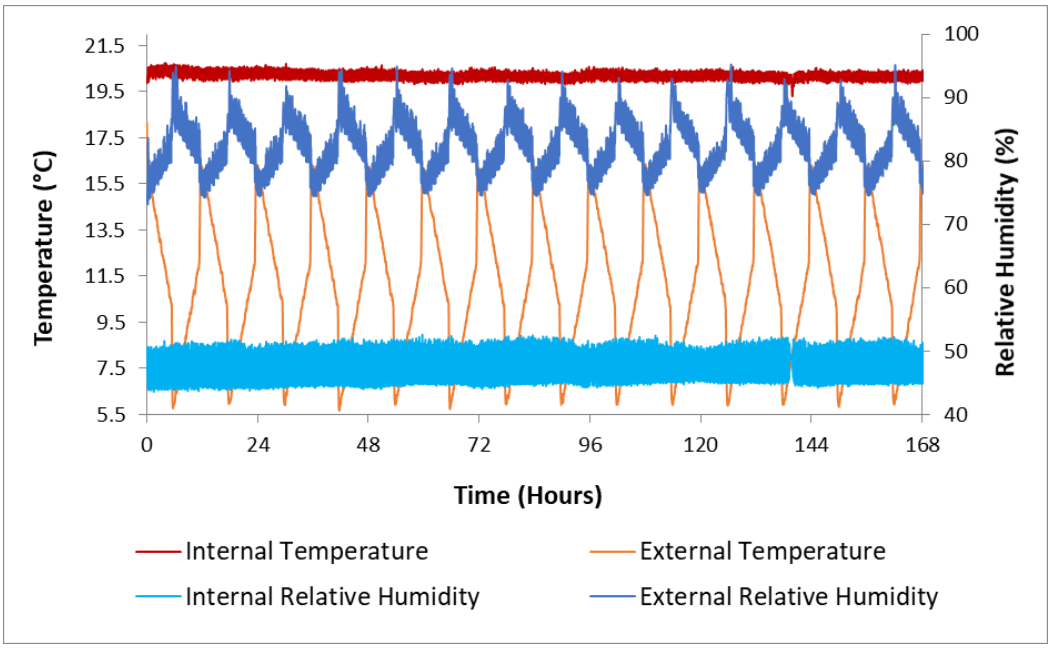

Figure 15. The winter dynamic profile in the environmental chamber.

Fig. 16 shows the running U-value and Fig. 17 shows the average U-value of the test panels, respectively. The averages U-values of Mineral Wool and Biond panels are within the error range of the designed U-value of the panels of 0.15 W/m^{2}K. The upper limit of the U-value of the Wood Fibre panels is 9.6% lower than the design U-value.

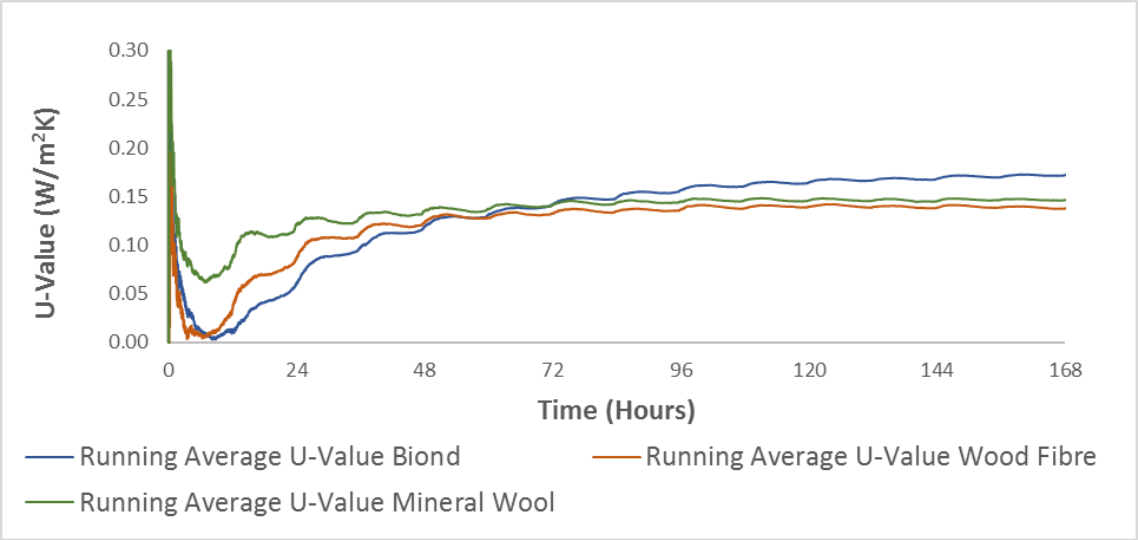

Fig. 16. The running U-Value of the panels during the winter dynamic test.

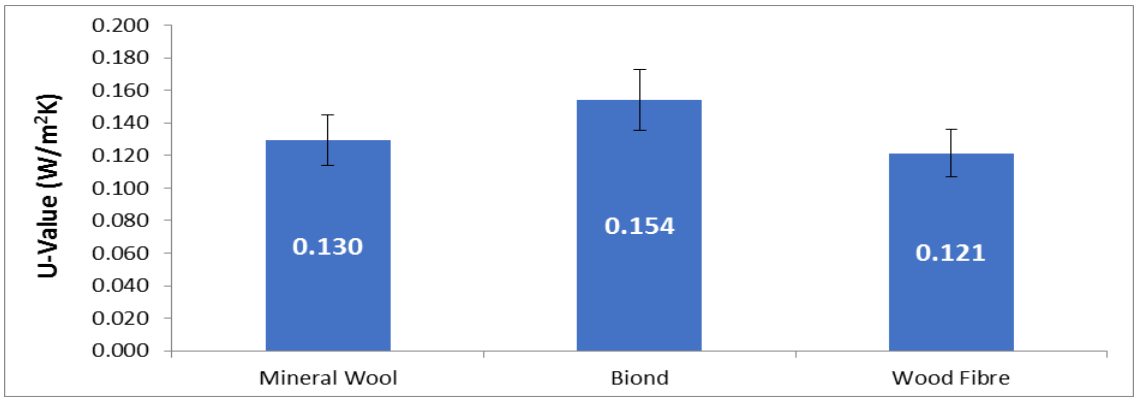

Fig. 17. The average U-Value of the panels during the winter dynamic test.

Since the slope of the vapour pressure gradient between the interior and exterior was alternating, its effect on heat flux was also assessed. (Fig. 18). No noticeable effect of vapour pressure gradient on heat flux was observed.

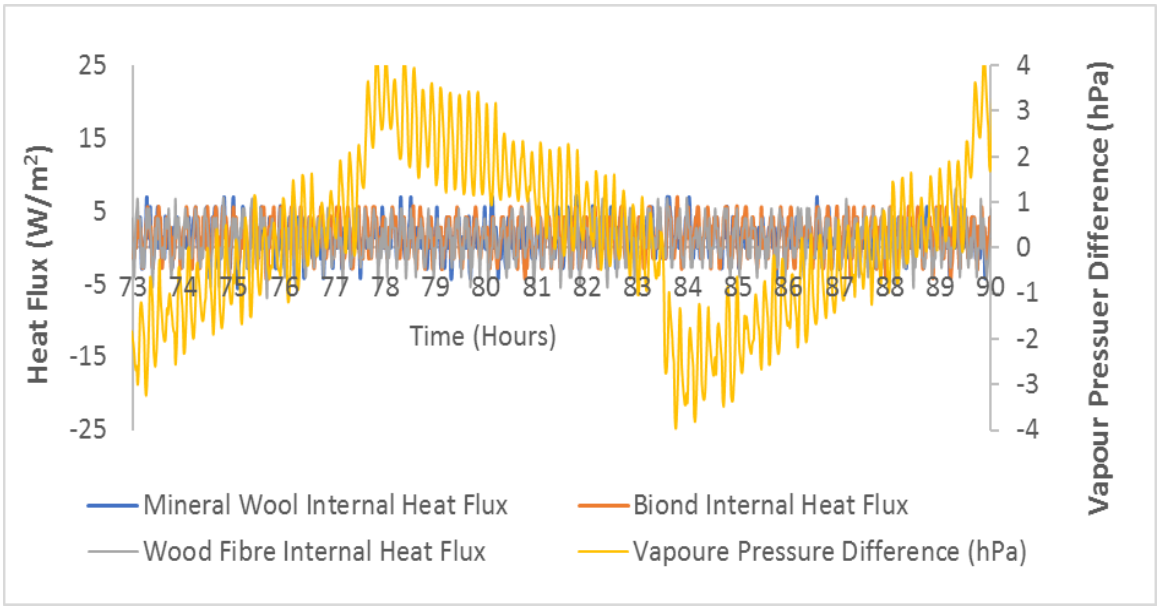

Fig.18. Heat flux in the internal surfaces and vapour pressure difference between the interior and the exterior.

Finally, relative humidity and vapour pressure at the centre of the panels were analysed (Fig. 19). The respective average relative humidity at the centre of Mineral Wool, Biond and Wood Fibre panels was 67%, 78% and 77% with the dew point temperature of 10.4°C, 12.1° C and 10.9°C respectively. As mentioned earlier, unlike the Mineral Wool panel that contains a vapour barrier, the other two panels are vapour open, and moisture propagation through them are managed by their moisture management capacities. For this reason, 10-11% higher relative humidity in those panels than that in the Mineral Wool panel is not unlikely.

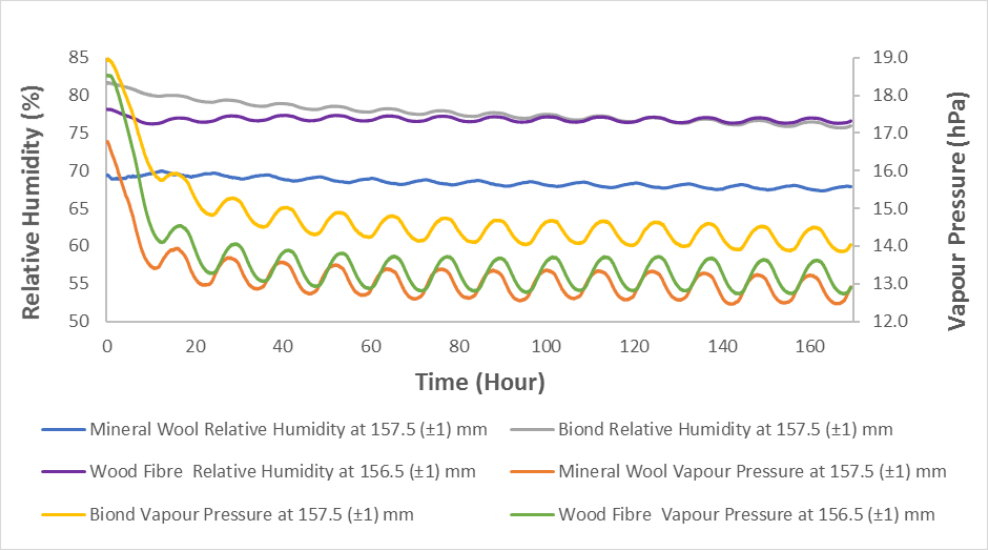

Fig. 19. Relative humidity and vapour pressure at the centre of the panels.

3.3. Thermal response test

The aim of the thermal response test was to compare the effect of thermal inertia of the wall panels. To this end, an intermittent internal heating regime was established. The internal temperature was set at 30 °C for 12 hours and 15 °C for 12 hours while the external temperature was kept constant at 15 °C so that the direction of heat flow cannot be outward during the second half of the cycle. No relative humidity profile was set, and as a result, the relative humidity in the chambers was uncontrolled.

The thermal response profile that was practically achieved by the environmental chamber is shown in Fig.20. It can be observed that the change in temperature from 30°C to 15 °C was attained in 6 hours as a steep ramp function instead of a step change. This was due to the inability of the environmental chamber to instantly attain the value of 15 °C. Furthermore, the exterior temperature varied between 16 °C and 16.3°C instead of remaining at a steady 15 °C. As a result, there was a temperature difference of 0.8 °C between the interior and exterior when the interior temperature was at its minimum. These caused a potential of heat flow from the exterior to the interior which was corrected during the data analysis.

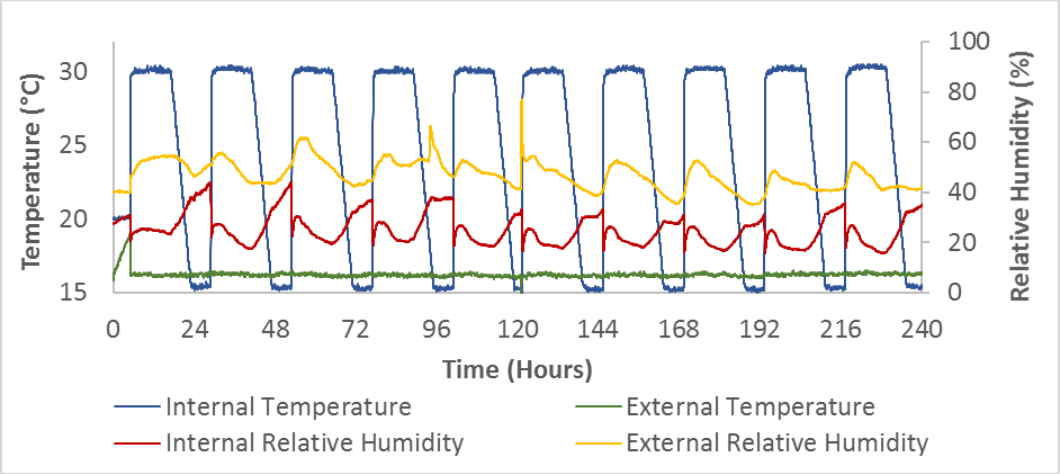

Figure 20. The thermal response temperature profile in the environmental chamber, relative humidity is uncontrolled (240 hours' data is presented).

Heat flux through panels during two typical stable temperature cycles are presented in Fig. 21.

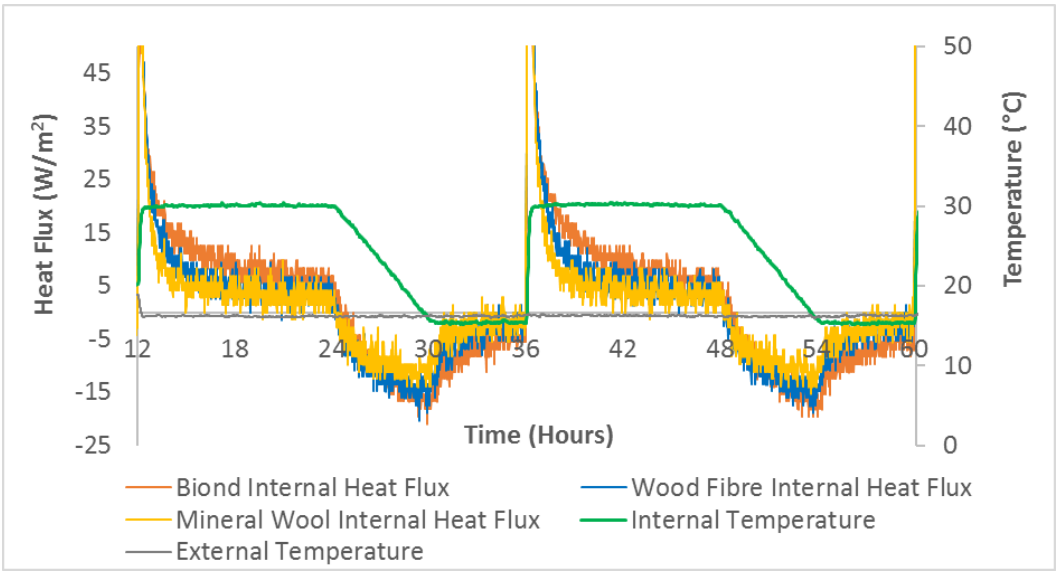

Fig. 21. Typical heat flux and temperature profile during the thermal response test.

The results of the analysis are presented in Fig. 22 in heat flux terms (W/m^2) and in Fig. 23 in energy terms (Wh) for a 24-hour cycle. It can be observed that the 'heat sink' is higher in the Biond panel than in the Mineral Wool and Wood Fibre panels by 84% and 42%, respectively. The 'heat retained in the system' is higher in the Biond panel

than in the Mineral Wool and Wood Fibre panels by 220% and 268%, respectively. It can also be noticed that, while outward heat flux from inside surface is highest in the Biond panel, the net 'outward heat flux' from outside is lower in the Biond panel than that in the Mineral Wool and Wood Fibre panels by 8% and 12%., respectively. Thus, when the panels are not in thermal equilibrium with the boundary conditions, internal heat flux sensors may overestimate the rate of heat loss from the panels.

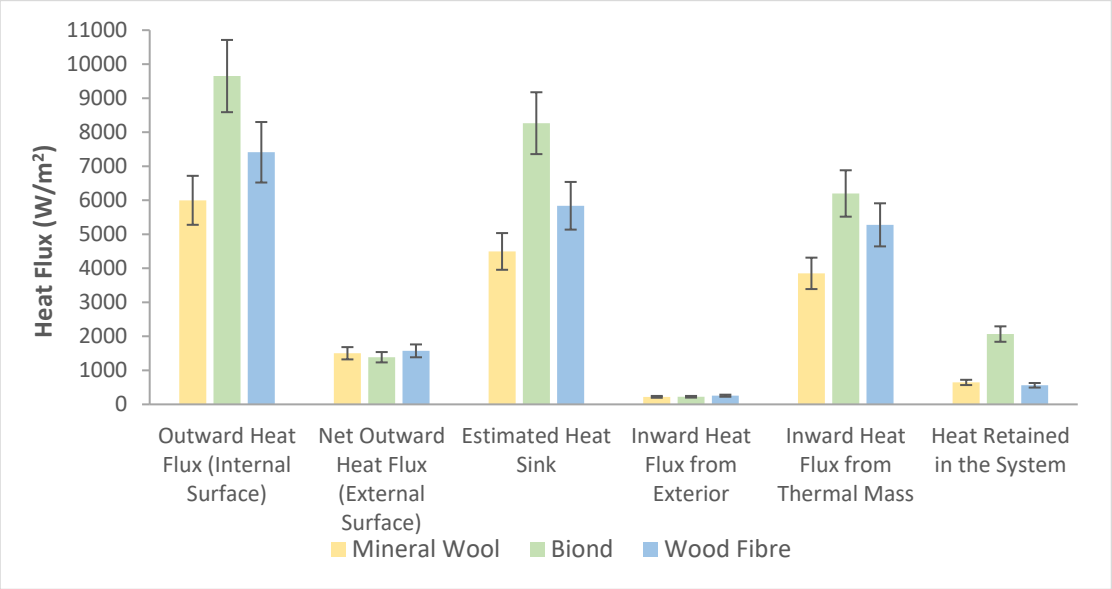

Fig.22. Thermal response of the panels in a 24-hour cycle.

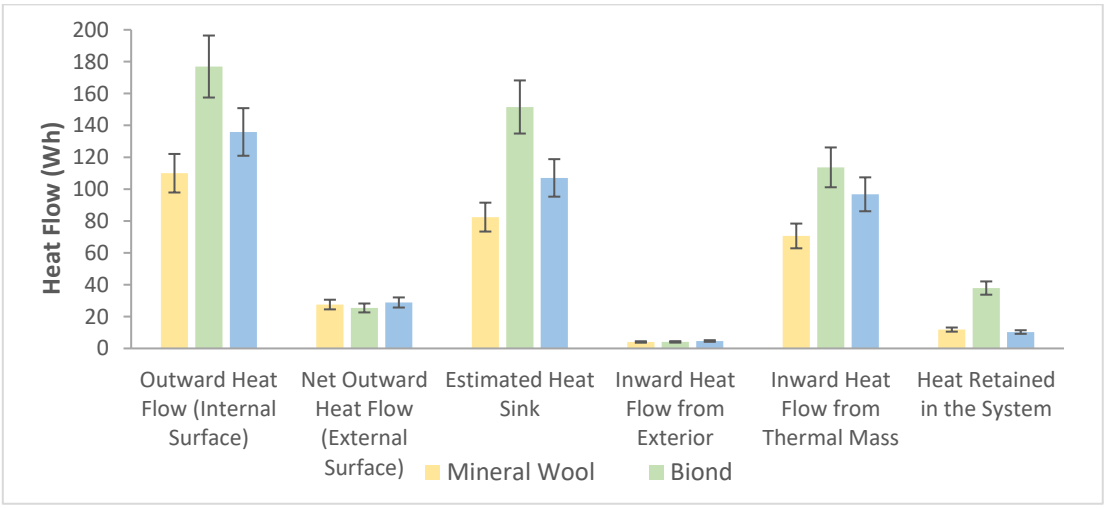

Fig. 23. Thermal response of the panels in energy terms in a 24-hour cycle.

The data are further analysed to understand the thermal inertia effect of the panels. The temperature evolution along the depth of the panels is compared during the following states of one typical thermal cycle:

1. Heating up period: The internal and external temperatures are set to 30°C and 15°C, respectively, as shown in Figs. 24-26.
2. Cooling down period: The internal temperature decreases from 30°C to 15°C and stays at 15 °C while the external temperature is set to 15°C as shown in Figs. 27-29.

Figs. 24-26 show that the Mineral Wool panel attains the steady state heat flow in 6 hours whereas the Biond and Wood Fibre panels are yet to reach steady state in 11 hours. It is plausible that the Biond and Wood Fibre panels continue absorbing heat due to their higher volumetric heat capacity.

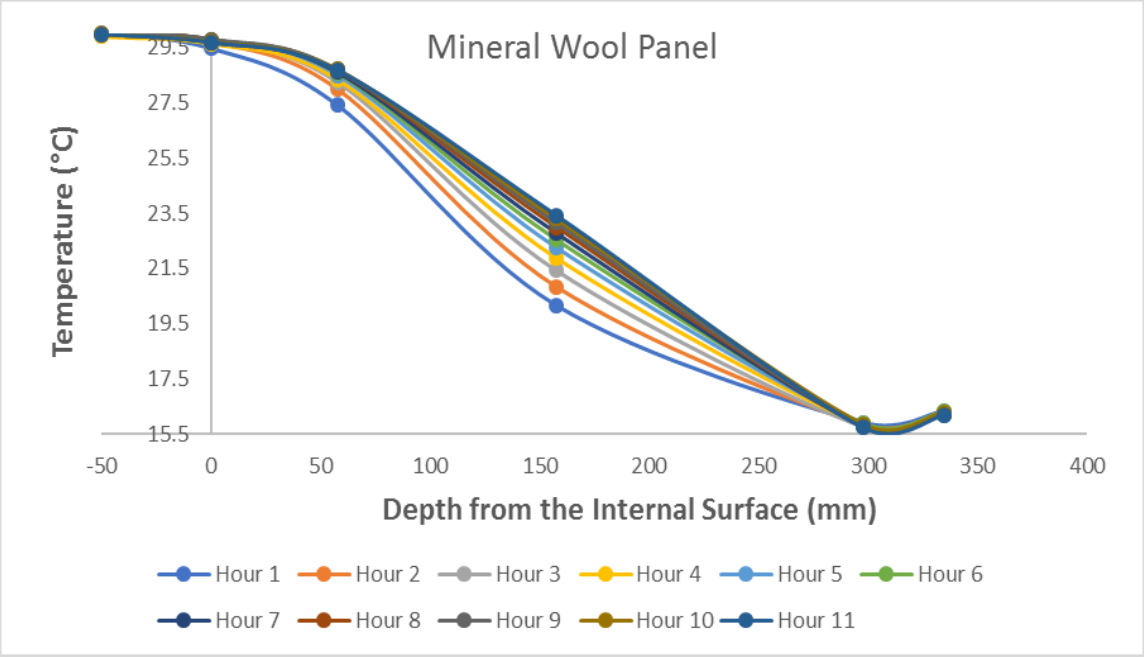

Fig. 24. The evolution of temperature gradient along the depth of the Mineral Wool panel during heating up.

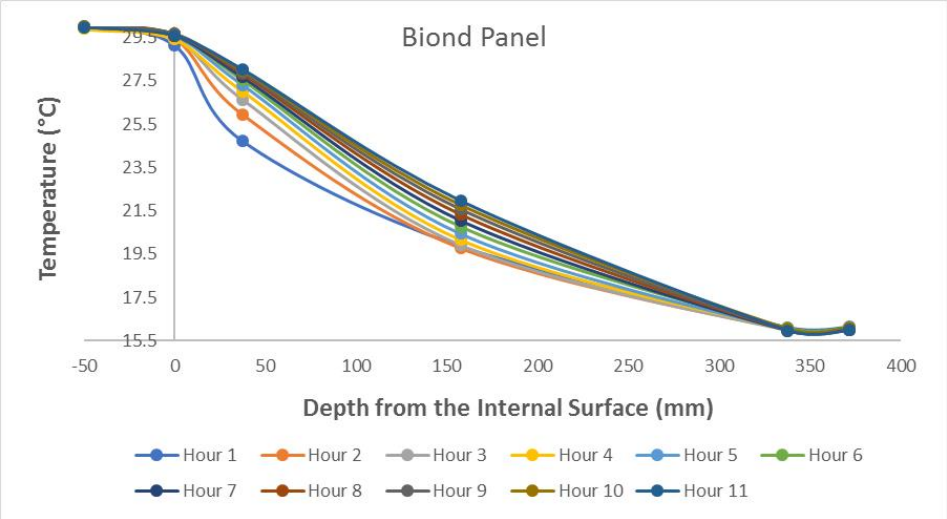

Fig. 25. The evolution of temperature gradient along the depth of the Biond panel during heating up.

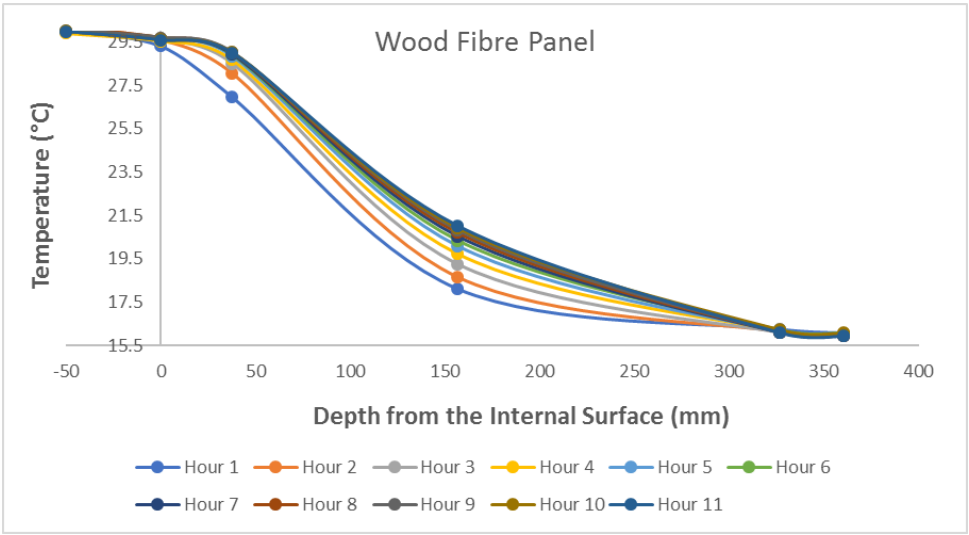

Fig. 26 The evolution of Temperature gradient along the depth of the Wood Fibre panel during heating up.

In Figs. 27-29, thermal inertia effects of the panels are compared in two ways. Firstly, the influence of the variability of the interior surface temperature of the panels between the 1st hour and the 9th hour on the variability in the temperature near the centre of the panels were assessed. Materials with higher thermal inertia respond to the changes in boundary temperature at a slower rate compared to the materials with lower thermal inertia. It can be observed that the temperature variability at the centre of the Mineral

Wool, Biond and Wood Fibre panels are 30%, 9% and 18%, respectively. Secondly, the thermal evolution along the depth of the panels was compared once the temperature of both sides of the panels was equal (±1°C). It can be observed that the ranges of temperature difference ΔT between the centre of the panels and the interior surface during hour 7 to hour 12 were 4.85 °C to 2.82 °C, 5.98 °C to 4.34 °C and 3.99 °C to 2.36 °C, respectively for Mineral Wool, Biond and Wood fibre panels.

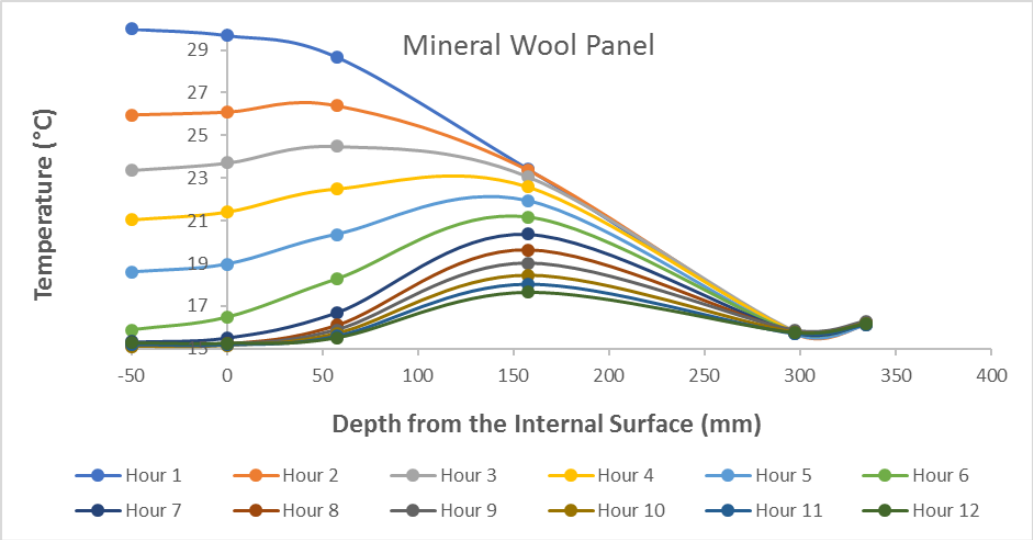

Fig. 27. Evolution of Temperature gradient along the depth of the Mineral Wool panel during cooling down.

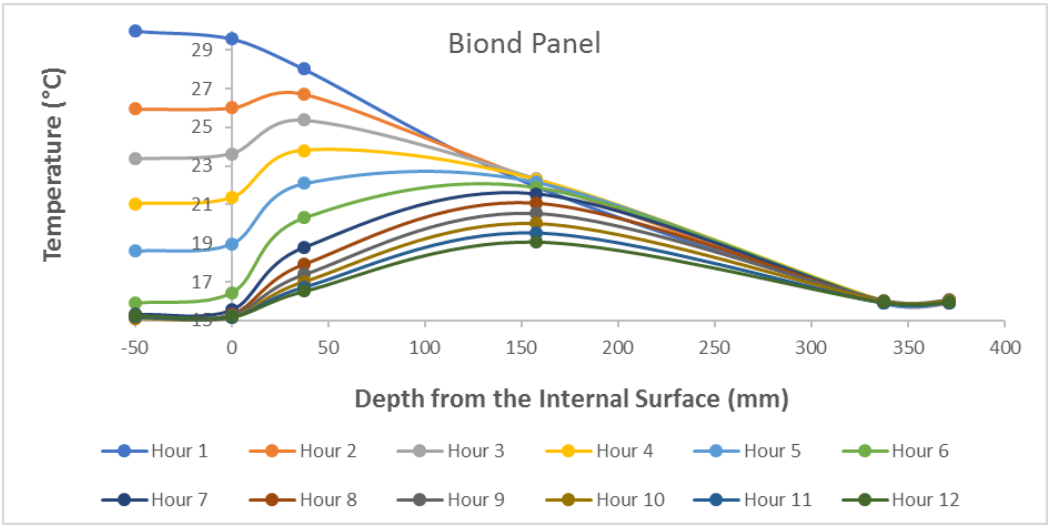

Fig. 28. Evolution of Temperature gradient along the depth of the Biond panel during cooling down.

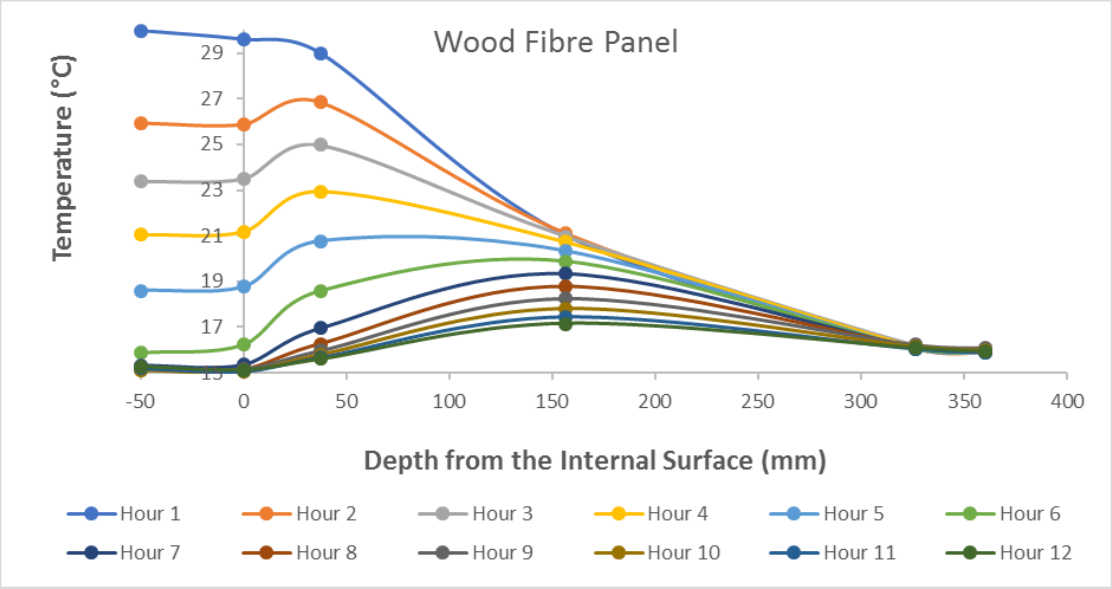

Fig. 29. Evolution of Temperature gradient along the depth of the Wood Fibre panel during cooling down.

Effective heat capacity is analytically assessed in terms of equivalent heat capacity [37], using Equation [9], Thermal Time Constant [38], using Equation [11] and [12] and effective thickness [39]. The findings are presented in Table 3. It can be observed that the measured thermal capacity values during one heating-up cycle is in good agreement with the Calculated effective thermal capacity (100mm).

Table 3. Calculated and measured thermal response properties of the panels.

	Calculated Equivalent heat capacity $(\rho.c)_{eq}$, (J/m^3k)	Calculated Thermal Time Constant $(TTC)_A$, (Hr)	Calculated Total Thermal Mass Q_m (Wh/k), based on $(TTC)_A$,	Measured effective Thermal Mass, (Wh/k)	Calculated effective thermal capacity (100mm), (J/m^2k)	Measured thermal capacity, one heating up cycle (J/m^2k)
Mineral Wool	148519	48	8.7	6.0	16932	19647
Biond	248911	128	23.3	11.0	38199	36120
Wood Fibre	194969	85	15.3	7.8	24348	25511

During this experiment, the fluctuation of vapour pressure and relative humidity in different depths of the panels in response to the fluctuating interior temperature were measured with specific emphasis on the centre of the panels along the depth. The fluctuation at the centre was the lowest in the Biond panel (Fig. 30), plausibly due to the high hygric and thermal inertia of the hemp-lime layer. Conversely, the Mineral Wool Panel demonstrated the highest degree of relative humidity and vapour pressure fluctuation at the centre. Since mineral wool incorporated a vapour barrier in front of the inner surface of the insulation, the level of relative humidity and vapour pressure were the lowest in the Mineral Wool Panel. Therefore, the higher fluctuation of vapour pressure and relative humidity is plausibly due to the low thermal and negligible hygric inertia of Mineral Wool. The risk of overheating of buildings due to global warming [61, 62] and the potential of controlled application of thermal mass, among other measures, in managing overheating of buildings is well documented [63-65]. In this respect, the role of envelope systems such as the Biond panel as a hybrid of thermal mass and thermal insulation requires further investigation.

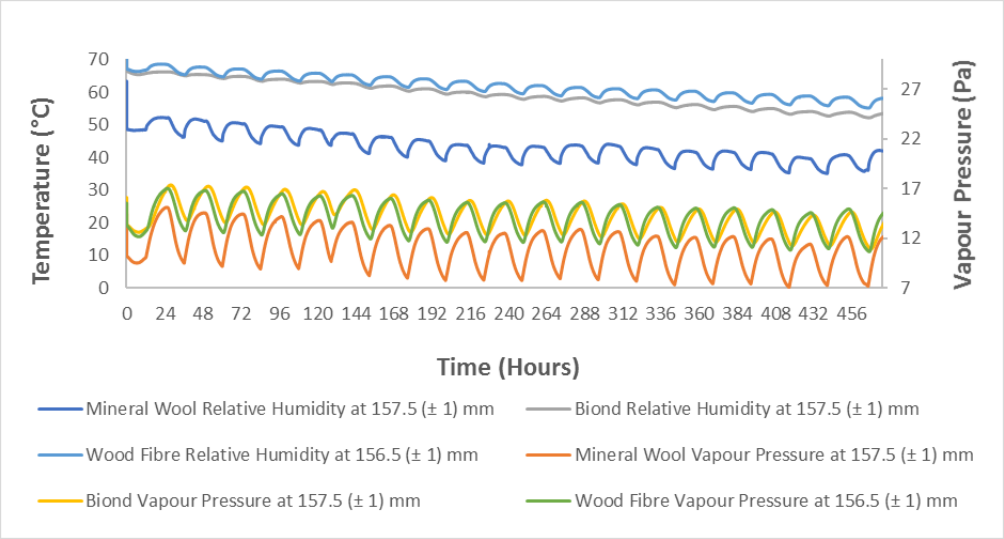

Fig. 30. Relative humidity and vapour pressure at the centre of Biond, Mineral Wool and Wood Fibre panels.

4. Conclusions

Three experimental tests were carried out in a large environmental chamber to assess the U-value, thermal inertia and hygric response of Biond, Wood Fibre and Mineral Wool panels under controlled environmental conditions. One steady state and one dynamic profile were used for the U-value analysis. During those tests, it was observed that the average U-Value of hemp-based 'Biond' test panel and the other two panels were within the error range of the corresponding design U-value (0.15 W/m^2K) of the panels. It implies that, unlike the Mineral Wool Panel, the other two cellulose based panels performed nearly to their designed standard without a vapour barrier such as that used in the mineral wool panel. However, the role of the inner linings such as plasterboard or OSB in controlling moisture flow cannot be ignored either. When it comes to the thermal response of the panels in intermittent heating profile, Biond demonstrated higher capacity than the other panels both in retaining and releasing heat in response to the interior temperature fluctuation. This characteristic of the Biond Panel is useful in maintaining hygrothermally stable room conditions that may eventually contribute to the higher level of occupant thermal comfort and reduced occurrences of overheating. The study emphasises the fact that the panels with high hygric and thermal inertia such as Biond or Wood Fibre need to be assessed in terms of their U-value, thermal inertia and hygric response to evaluate their operational hygrothermal performance. The paper did not study some aspects of heat and moisture transfer during the experiments such as the edge effect, the total moisture content in the panels at the beginning and end of the tests in terms of gravimetric measurement. These limitations need to be addressed in any future research.

Acknowledgements

This publication has been produced with the assistance of the European Union [grant

number ECO/12/332972/SI2.653796- HEMPSEC]. The contents of this publication are the sole responsibility of the authors and can in no way be taken to reflect the views of the European Union.

References

[1] H. Ma, W. Zhou, X. Lu, Z. Ding, Y. Cao, Application of Low Cost Active and Passive Energy Saving Technologies in an Ultra-low Energy Consumption Building, Energy Procedia 88 (2016) 807-813.
[2] BRE, What is BREEAM?, 2017. http://www.breeam.com/. (Accessed 01/08/2017 2017).
[3] USGBC, Better Buildings are our Legacy, 2017. https://www.usgbc.org/leed. (Accessed 1/08/2017 2017).
[4] IBEC, CASBEE Basic Concept, 2017. http://www.ibec.or.jp/CASBEE/english/basicconceptE.htm. (Accessed 01/08/2017 2017).
[5] F. Aldawi, F. Alam, A. Date, M. Alghamdi, F. Aldhawi, A new house wall system for residential buildings, Energy and Buildings 67 (2013) 403-418.
[6] PHI, About Passive House - What is a Passive House? http://www.passiv.de/en/02_informations/01_whatisapassivehouse/01_whatisapassivehouse.htm. (Accessed 01/08/2017 2017).
[7] Minergie, Mit Minergie-P zertifizieren, (2017).
[8] J. Zach, A. Korjenic, V. Petránek, J. Hroudová, T. Bednar, Performance evaluation and research of alternative thermal insulations based on sheep wool, Energy and Buildings 49 (2012) 246-253.
[9] BRE, BREEAM In-Use International Technical Manual, BRE, Watford, UK, 2016.
[10] DCLG, Improving the energy efficiency of our buildings: A guide to display energy certificates and advisory reports for public buildings, in: D.f.C.a.L. Government (Ed.) Department for Communities and Local Government, London, 2015.
[11] O. Guerra-Santin, C. Tweed, H. Jenkins, S. Jiang, Monitoring the performance of low energy dwellings: Two UK case studies, Energy and Buildings 64 (2013) 32-40.
[12] A. Stafford, D. Johnston, D. Miles-Shenton, D. Farmer, M. Brooke-Peat, C. Gorse, Adding value and meaning to coheating tests, Structural Survey 32(4) (2014) 331-342.
[13] H. Monteiro, F. Freire, Life-cycle assessment of a house with alternative exterior walls: Comparison of three impact assessment methods, Energy and Buildings 47 (2012) 572-583.
[14] R. Galvin, Making the 'rebound effect' more useful for performance evaluation of thermal retrofits of existing homes: Defining the 'energy savings deficit' and the 'energy performance gap', Energy and Buildings 69 (2014) 515-524.
[15] P. deWilde, The gap between predicted and measured energy performance of buildings: A framework for investigation, Automation in Construction 41 (2014) 40-49.
[16] D. Cal`ı, T. Osterhage, R. Streblow, D. Muller, Energy performance gap in refurbished German dwellings: lesson learned from a field test, Energy and Buildings (2016).
[17] T. Wei, Y. Liu, Estimation of global rebound effect caused by energy efficiency improvement, Energy Economics 66 (2017) 27-34.

[18] T.R. Whiffen, G. Russell-Smith, S.B. Riffat, Active thermal mass enhancement using phase change materials, Energy and Buildings 111 (2016) 1-11.
[19] S.A. Al-Sanea, M.F. Zedan, S.N. Al-Hussain, Effect of thermal mass on performance of insulated building walls and the concept of energy savings potential, Applied Energy 89(1) (2012) 430-442.
[20] L. Yang, Y. Li, Cooling load reduction by using thermal mass and night ventilation, Energy and Buildings 40(11) (2008) 2052-2058.
[21] Y. Goto, K.G. Wakili, Y. Ostermeyer, T. Frank, N. Ando, H. Wallbaum, Preliminary investigation of a vapor-open envelope tailored for subtropical climate, Building and Environment 46(3) (2011) 719-728.
[22] Z. Pavlík, J. Žumár, I. Medved, R. Černý, Water Vapor Adsorption in Porous Building Materials: Experimental Measurement and Theoretical Analysis, Transport in Porous Media 91(3) (2011) 939-954.
[23] L. Arnaud, Comparative study of hygrothermal Performances of building materials, NOCMAT 2009: the 11th International Conference on Non-conventional Materials and Technologies, Bath, UK, 2009.
[24] E. Latif, S. Tucker, M.A. Ciupala, D.C. Wijeyesekera, D.J. Newport, M. Pruteanu, Quasi steady state and dynamic hygrothermal performance of fibrous Hemp and Stone Wool insulations: Two innovative laboratory based investigations, Building and Environment 95 (2016) 391-404.
[25] E. Latif, M.A. Ciupala, D.C. Wijeyesekerac, The comparative in situ hygrothermal performance of Hemp and Stone Wool insulations in vapour open timber frame wall panels, Construction and Building Materials 73 (2014) 205-213.
[26] A. Nicolajsen, Thermal transmittance of a cellulose loose-fill insulation material, Building and Environment 40 (2005) pp. 907-914.
[27] J.R. Southern, Summer condensation within dry lined solid walls, Building Services Engineering Research and Technology 7(3) (1986) 101-106.
[28] R. Walker, S. Pavía, Thermal performance of a selection of insulation materials suitable for historic buildings, Building and Environment 94 (2015) 155-165.
[29] A. Shea, M. Lawrence, P. Walker, Hygrothermal performance of an experimental hemp–lime building, Construction and Building Materials 36 (2012) 270-275.
[30] R. McClung, H. Ge, J. Straube, J. Wang, Hygrothermal performance of cross-laminated timber wall assemblies with built-in moisture: field measurements and simulations, Building and Environment 71 (2014) 95-110.
[31] F. Stazi, F. Tittarelli, G. Politi, C. Di Perna, P. Munafò, Assessment of the actual hygrothermal performance of glass mineral wool insulation applied 25 years ago in masonry cavity walls, Energy and Buildings 68 (2014) 292-304.
[32] S. Tucker, E. Latif, D.C. Wijeyesekera, D. Ahadzie, An experimental study of moisture buffering of bio-insulations in lofts, Structural Survey 32(5) null.
[33] J. Toman, A. Vimmrová, R. Černý, Long-term on-site assessment of hygrothermal performance of interior thermal insulation system without water vapour barrier, Energy and Buildings 41(1) (2009) 51-55.
[34] F. Collet, J. Chamoin, S. Pretot, C. Lanos, Comparison of the hygric behaviour of three hemp concretes, Energy and Buildings 62 (2013) 294-303.
[35] F. Collet, S. Pretot, Experimental highlight of hygrothermal phenomena in hemp concrete wall, Building and Environment 82 (2014) 459-466.
[36] S.P. Florence Collet, Experimental investigation of moisture buffering capacity of sprayed hemp concrete, Construction and Building Materials 36 (2012) 58-65.
[37] R. Bevan, T. Woolley, Hemp lime construction : a guide to building with hemp lime composites, IHS BRE Press, Bracknell, 2008.

[38] P. Daly, P. Ronchetti, T. Woolley, Hemp Lime Bio-composite as a Building Material Irish Construction, Environmental Protection Agency, Ireland, 2012.
[39] F. Collet, F. Achchaq, K. Djellab, B.H. Marmoret, Water vapor properties of two hemp wools manufactured with different treatments, Construction and Building Materials 25 (2011) 1079-1085.
[40] E. Latif, M. Lawrence, A. Shea, P. Walker, In situ assessment of the fabric and energy performance of five conventional and non-conventional wall systems using comparative coheating tests, Building and Environment 109 (2016) 68-81.
[41] Rockwool, RAINSCREEN DUO SLAB® Non-combustible thermal insulation, (2017).
[42] T.L. Company, Hempcrete Factsheet, 2017. http://limecrete.co.uk/hempcrete-factsheet/.
[43] Pavatex, PAVAFLEX Flexible woodfibre insulation material, 2017. https://www.mikewye.co.uk/product/pavaflex-flexible-wood-fibre-insulation/.
[44] Pavatex, Pavadentro: Internal Woodfibre Insulation, 2017. http://www.pavatex.com/en/products/wall/pavadentro. (Accessed 07/12/2917 2017).
[45] Ł. Czajkowski, W. Olek, J. Weres, R. Guzenda, Thermal properties of wood-based panels: specific heat determination, Wood Science and Technology 50(3) (2016) 537-545.
[46] S. Wood, Properties of softwood, 2017. file:///C:/Users/eshra/Desktop/Properties%20of%20softwood%20-%20Swedish%20Wood.html. 2017).
[47] B. Gypsum, Environmental Product Declarartion: 12.5mm Gyproc WallBoard. file:///C:/Users/eshra/Documents/Downloads/EPD-12-5mm-Gyproc-WallBoard.pdf. (Accessed 11.12.17 2017).
[48] T.E. Toolbox, Air Properties, 2017. https://www.engineeringtoolbox.com/air-properties-d_156.html.
[49] B. Anderson, Conventions for U-value calculations, Bracknell, UK, 2006.
[50] Campbell, CS215 Temperature and Relative Humidity Probe, 2017. http://s.campbellsci.com/documents/af/manuals/cs215.pdf. (Accessed 26/12/2017 2017).
[51] R. Components, Cable Selection Guide, 2017. http://docs-europe.electrocomponents.com/webdocs/15e5/0900766b815e5303.pdf. (Accessed 22/12/2017 2017).
[52] Hukseflux, HFP01 Heat flux plate, 2016. http://www.hukseflux.com/product/hfp01?referrer=/product_group/heat-flux-sen. (Accessed 10.09.16 2016).
[53] B.S. Institute, BS EN ISO 6946. Building components and building elements. Thermal resistance and thermal transmittance. Calculation method, 2007.
[54] E. Latif, M.A. Ciupala, S. Tucker, D.C. Wijeyesekera, D.J. Newport, Hygrothermal performance of wood-hemp insulation in timber frame wall panels with and without a vapour barrier, Building and Environment 92 (2015) 122-134.
[55] BS ISO 9869-1:2014. Thermal insulation-Building elements -In-situ measurement of thermal resistance and thermal transmittance, The British Standards Institution, United Kingdom, 2014.
[56] ISO 9869. Thermal insulation-Building elements -In-situ measurement of thermal resistance and thermal transmittance, International Organization for Standardization, Switzerland, 1994.
[57] P.T. Tsilingiris, On the thermal time constant of structural walls, Applied Thermal Engineering 24(5-6) (2004) 743-757.

[58] B. Givoni, Climate Considerations in Building and Urban Design, Van Nostrand Reinhold : John Wiley1998.
[59] B.S. Institute, BS EN ISO 13786. Thermal performance of building components - Dynamic thermal characteristics - Calculation methods, BSI, 2017.
[60] E. Latif, M. Lawrence, A. Shea, P. Walker, Moisture buffer potential of experimental wall assemblies incorporating formulated hemp-lime, Building and Environment 93 (2015) 199-209.
[61] A.D. Peacock, D.P. Jenkins, D. Kane, Investigating the potential of overheating in UK dwellings as a consequence of extant climate change, Energy Policy 38(7) (2010) 3277-3288.
[62] E. Oikonomou, M. Davies, A. Mavrogianni, P. Biddulph, P. Wilkinson, M. Kolokotroni, Modelling the relative importance of the urban heat island and the thermal quality of dwellings for overheating in London, Building and Environment 57 (2012) 223-238.
[63] N. Arcuri, C. Carpino, M. De Simone, The Role of the Thermal Mass in nZEB with different Energy Systems, Energy Procedia 101 (2016) 121-128.
[64] T.O. Adekunle, M. Nikolopoulou, Thermal comfort, summertime temperatures and overheating in prefabricated timber housing, Building and Environment 103 (2016) 21-35.
[65] R. Ponechal, Increasing Thermal Mass in Low Carbon Dwelling, Procedia Engineering 111 (2015) 645-651.